Available online at www.sciencedirect.com
ScienceDirect
Tunnelling and Underground Space Technology xxx (2007) xxx–xxx
Tunnelling and Underground Space Technology
incorporating Trenchless Technology Research
www.elsevier.com/locate/tust

Lining design for the district heating tunnel in Copenhagen with steel fibre reinforced concrete segments

Thomas Kasper [a,*], Carola Edvardsen [a], Gert Wittneben [b], Dieter Neumann [b]

[a] COWI A/S, Parallelvej 2, 2800 Kongens Lyngby, Denmark
[b] HOCHTIEF Construction AG, Alfredstrasse 236, 45133 Essen, Germany

Received 22 April 2007; received in revised form 30 October 2007; accepted 2 November 2007

Abstract

The 3.9 km long district heating tunnel carries heating pipelines from a power plant on the island Amager into the centre of Copenhagen. A shaft on Amager and two shafts in the city centre provide access to the tunnel, which is located within the Copenhagen limestone at a depth between 25 and 38 m below the ground surface. The tunnel is excavated with an earth pressure balance (EPB) shield machine and is lined with steel fibre reinforced concrete (SFRC) segments without any conventional steel bar reinforcement. This represents an advantageous and innovative technical as well as cost-efficient solution. This paper presents the methods applied in the structural and durability design of the SFRC segmental lining for a specified service life of 100 years. Special attention is required due to the temperature increase in the tunnel to approximately 50 °C during operation of the pipelines. The experiences with the SFRC segments during construction of the tunnel are discussed.

Keywords: Steel fibre reinforced concrete; SFRC; Tunnel lining; Segment design; Durability design

1. Introduction

Steel fibre reinforced concrete (SFRC) has been a subject of research for several decades (see e.g. Maidl, 1995). Steel fibres introduce a ductile post-cracking and a favourable crack distribution behaviour of the concrete. Due to the fact that they do not require a concrete cover, they help to prevent local damage like wear, spalling at edges and chipping of corners. Furthermore, they increase the impact resistance of the concrete. One major advantage of SFRC compared to conventionally reinforced concrete is its corrosion resistance and the resulting improved durability. Although individual fibres close to the surface can rust (which may give an aesthetic problem), the corrosion cannot propagate. SFRC is further characterised by low production costs, which is particularly relevant for lining segments with complicated and time-consuming reinforcement cages. Despite these favourable properties it has to be noted that SFRC cannot compete with conventionally reinforced concrete in terms of bending and tension capacity as well as bursting capacity under concentrated large loads.

The final loading situation of circular, segmental tunnel linings is typically characterised by the dominance of compressive normal forces combined with relatively small bending moments. This allows for the application of SFRC segments without conventional steel bar reinforcement. Compared to traditionally reinforced segments, no concrete cover is needed. If shear key or tongue and groove connections between the rings can be avoided e.g. by a grout solution which ensures quick stabilization of the lining rings, this enables a possible thickness reduction of the segments. It should be noted, however, that the economically and technically attractive SFRC solution requires special considerations and care with regard to the temporary

* Corresponding author. Tel.: +45 45972211; fax: +45 45972212.
E-mail addresses: tkas@cowi.dk (T. Kasper), cle@cowi.dk (C. Edvardsen), gert.wittneben@hochtief.de (G. Wittneben), dieter.neumann@hochtief.de (D. Neumann).

0886-7798/$ - see front matter © 2007 Elsevier Ltd. All rights reserved.
doi:10.1016/j.tust.2007.11.001

loading situations during segment production, transport, installation and tunnel drive and with regard to the concentrated load transfer at the radial joints in the final situation.

Steel fibre reinforcement has frequently been used for precast segmental tunnel linings in combination with conventional steel bar reinforcement. However, only relatively few applications of SFRC segments without any conventional reinforcement have been reported in the literature so far. To the authors' knowledge, this type of lining was first used in a 1.5 km long baggage handling tunnel at London Heathrow Airport (Moyson, 1995; Anonymous, 1995). A test application in 140 m of a pressurized water tunnel in the Lesotho Highlands Water Project in South Africa was motivated by the corrosion resistance and the expected long-term repair savings. This project was accompanied by an extensive research, testing and monitoring programme (Wallis, 1995; Viljoen et al., 1995). Within a pilot project in the Netherlands, 16 rings of the 2. Heinenoord Tunnel were made of SFRC segments (Kooiman et al., 1999) and the first large scale application of SFRC segments was in approximately 20 km twin-tube sections of the Channel Tunnel Rail Link in England (Woods and Battye, 2003; Warren et al., 2003; Davis et al., 2006). In recent years, an increasing number of more detailed publications focussing on design methods and experimental investigations of SFRC segmental linings can be found (e.g. De Waal, 1999; Kooiman, 2000; Dupont et al., 2003; Suter and Bergmeister, 2004; Gettu et al., 2004; King, 2005; Woods et al., 2005; Dobashi et al., 2006; Plizzari and Tiberti, 2006; Molins et al., 2006). Design guidelines for SFRC have been developed in several countries, but – although in progress – no standards are available yet.

This paper is concerned with the design of the tunnel lining for the district heating tunnel in Copenhagen, where steel fibres are used as the only reinforcement of the segments. Section 2 of this paper gives a short general overview of the project. The structural and durability design of the tunnel lining is presented in Sections 3 and 4, respectively. The subsequent Sections 5 and 6 are devoted to the gasket design and laboratory testing of the SFRC. Experiences gained during segment production and construction of the tunnel are summarised in Section 7. The paper closes with conclusions and future prospects in Section 8.

2. Project overview and design basis

The 3.9 km long district heating tunnel connects the power plant on the island Amager with the city centre of Copenhagen, Denmark (Fig. 1). The tunnel has an internal diameter of 4.2 m and carries two steam pipes, two hot water pipes and two condensation pipes. Located at a depth between 25 and 38 m below the ground surface, the tunnel is bored with an EPB shield machine through Copenhagen limestone. This type of TBM was also successfully used in the Copenhagen metro project (Nymann and Taylor, 2003). The geological conditions along the alignment of the tunnel are characterised by quarternary soft soil deposits down to depths between 14 and 18 m below the ground surface, followed by the Copenhagen limestone with different degrees of induration (Knudsen et al., 1995; Hansen and Foged, 2002; Jackson et al., 2004). The design groundwater levels range between 0 and 8 m below the ground surface. The tunnel is accessed via a 37 m deep shaft at the Amager power plant. It starts with a straight-line, 2.4 km long stretch with a downward inclination of 2‰ to the 44 m deep shaft at Adelgade, where it turns about 56° northwards and then continues in a 1.5 km long stretch with an upward inclination of 11‰ to the 30 m deep end shaft at Fredensgade. The alignment of the tunnel was chosen due to the favourable geological conditions in the middle Copenhagen limestone, to keep a minimum distance to the crossing future subway line close to the shaft at Adelgade and to keep required minimum inclinations to deal with condensates in the steam pipes during operation. Excavation in the limestone at large depth minimises the settlement risk of sensitive above-ground buildings and

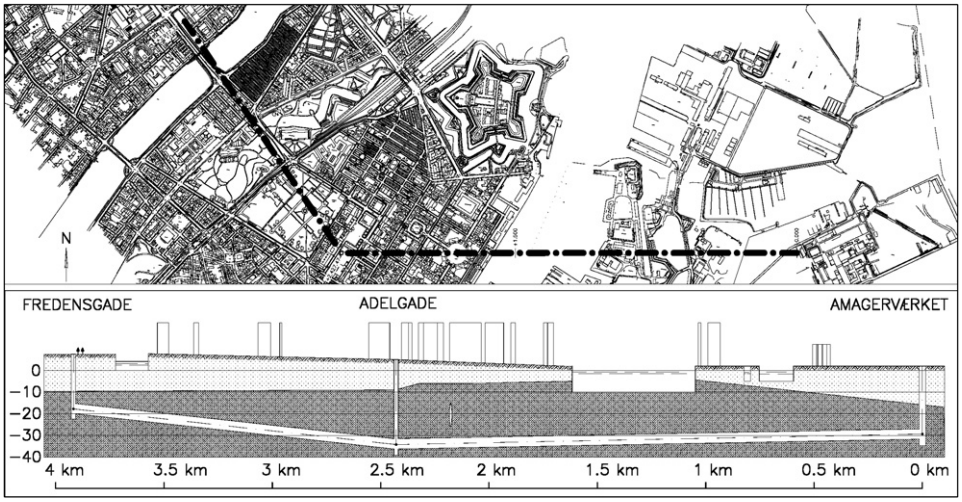

Fig. 1. Layout of the district heating tunnel in Copenhagen.

Please cite this article in press as: Kasper, T. et al., Lining design for the district heating tunnel in Copenhagen, Tunnel. Underg. Space Technol. (2007), doi:10.1016/j.tust.2007.11.001

infrastructure in case of shallow tunnelling in soft soils (Kasper and Meschke, 2006a,b). The upper parts of the shafts in the quarternary soft soil layers are constructed with secant pile walls down to a depth of 16 m at Adelgade, 20 m at Fredensgade and 27 m at the Amager plant. This was considered to be the best solution to excavate the shafts through aquifers containing flow zones and to minimise the excavation induced settlements of the ground surface. The lower parts of the shafts within the limestone are mined with excavators and temporarily lined with shotcrete. Short NATM tunnels are excavated from the shafts. These tunnels (10-17 m long) with a larger diameter than the bored tunnel are required for the pipeline installations and for the TBM launches. Both the shafts and the NATM caverns are finally lined with permanent reinforced concrete linings.

The design work for the tunnel started in October 2004 and the construction works for the shafts started in September 2005. The TBM began excavation from the shaft at the Amager power plant in June 2006 and finished its work in April 2007. The two sections Amagerværk – Adelgade and Adelgade – Fredensgade are due for operation of the pipelines end of December 2008 and end of March 2009, respectively. The total costs of the project are estimated to be DKK 750 million including the piping works.

It was decided to design the tunnel lining for the bored tunnel with SFRC segments without conventional steel bar reinforcement, using the German SFRC design guideline (DBV, 2001) as the design basis. The specified service life of the tunnel is 100 years.

3. Structural design

3.1. Lining characteristics

The tunnel lining has a thickness of 30 cm. The lining rings are 1.50 m wide and have a taper of 2 cm to allow for alignment corrections during construction. Each ring consists of three standard segments, two counter key segments and one key segment (Fig. 2). The lining has flat concrete-to-concrete radial joints and flat circle joints equipped with 450 × 175 mm, 0.9 mm thick bituminous packers. The joints are temporarily bolted with straight bolts in pockets. The specified material characteristics of the steel fibre reinforced concrete are summarised in Table 1. The steel fibres are 47 mm long, 0.8 mm diameter cold drawn wire steel fibres with hooked ends and profiled surface. The tensile strength parameters of the SFRC are determined in 4-point bending tests according to the German guideline (Fig. 3). The resulting idealised stress–strain diagram of the SFRC is shown in Fig. 4. In this Figure, ε_{ct}^{f} and σ_{ct}^{f} denote the tensile strain and stress, respectively. Cracking occurs at the tensile strength of the concrete f_{ctm}. The post-cracking behaviour is characterised by the equivalent strength parameters $f_{eq,ctk,I}$ (SLS), $f_{eq,ctd,I}$ (ULS) at deformation level I, i.e. shortly (0.1‰) after crack initiation, and the equivalent strength parameters $f_{eq,ctk,II}$ (SLS), $f_{eq,ctd,II}$ (ULS) at deformation level II, i.e. after large tensile strains (10‰).

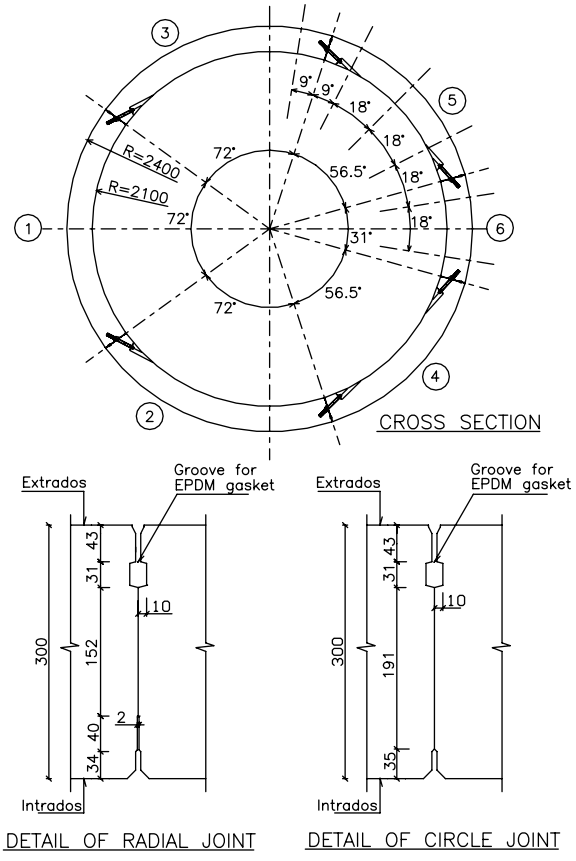

Fig. 2. Details of the segmental lining.

Table 1
Material characteristics of the steel fibre reinforced concrete for the tunnel lining

Concrete type, fibre concrete class	C50/60, F1.4/0.6
Unit weight (kN/m^3)	24
Young's modulus E (MPa)	36,800
Poisson's ratio (–)	0.17
Compressive strength (MPa)	50
Equivalent flexural tensile strength at deformation level I $f_{eq,ctk,I}$ (MPa)	1.4
Equivalent flexural tensile strength at deformation level II $f_{eq,ctk,II}$ (MPa)	0.6
Fibre type and dosage	DUOLOC 47/0.80 35 kg/m^3

3.2. Grout characteristics

The grout for the district heating tunnel is a two-component grout based on cement, bentonite, water and stabilizer as component A and water and sodium silicate (water glass) as component B. This innovative grout used to fill the 15 cm thick annular gap between the tunnel lining and the limestone behind the TBM is characterised by short gelling and setting time. This ensures a quick stabilization of the tunnel lining, avoids buoyancy induced uplift of the rings,

Please cite this article in press as: Kasper, T. et al., Lining design for the district heating tunnel in Copenhagen, Tunnel. Underg. Space Technol. (2007), doi:10.1016/j.tust.2007.11.001

Fig. 3. 4-Point bending test to determine the flexural tensile strengths of the SFRC according to the German guideline.

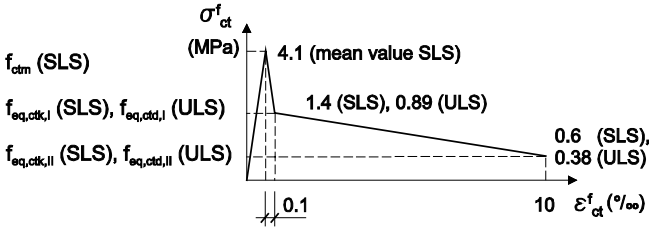

Fig. 4. Idealised stress–strain diagram according to the German guideline.

settlements due to the loads from the back-up trailer and the resulting shear displacements between the segments. The two-component grout thus forms the basis for high production rates. Conventional grout gains its early-age strength from consolidation (Bezuijen and Talmon, 2003; Talmon and Bezuijen, 2006). The grouting pressure causes a fluid loss of conventional grout into the surrounding soil. The associated decrease of the porosity and increasing grain-to-grain stresses lead to the formation of a layer of consolidated grout that grows from the surrounding soil towards the lining. A sufficiently high permeability of the ground forms the basis for this consolidation, which would not take place in the limestone with a low permeability of 1e−6 m/s. With a conventional grout, a coupling of the lining rings by means of shear key or tongue and groove connections would therefore be needed to avoid differential ring displacements in the unconsolidated, liquid grout. Transfer of larger shear forces through these connections between the rings requires a certain minimum thickness of the segments and would be difficult to achieve without steel bar reinforcement. A special requirement for the grout of the district heating tunnel is a relatively low final stiffness and strength to avoid too large thermal stresses in the operation phase of the tunnel (Section 3.8). This can be conveniently accomplished with the chosen two-component grout. The hardened grout has been tested in the laboratory at an age of 28 days showing a low scatter of properties with a unit weight of 12 kN/m^3, a Young's modulus of 1000 MPa and an unconfined compressive strength of 1.1 MPa. The Poisson's ratio is estimated to be 0.25.

3.3. Segment production and transport

The segments are produced in a precast factory in Berlin, Germany, in fixed steel moulds in the horizontal configuration with intrados down. The concrete mixer is a precast factory standard plant. To ensure the required uniform distribution and amount of the fibres in the fresh concrete they are added to the concrete mixer via air stream with a continuous weighing system. The moulds are equipped with a vibrator. The duration and frequency of vibration have been optimized to maintain an even fibre distribution and to avoid segregation, which have been investigated by means of petrographic analyses. After having reached a required minimum compressive strength of 20 MPa after 12 h, the segments are demoulded with a vacuum lifting device. They are stored and covered for 24 h in the production hall. During that time, the necessary reworking (cosmetic repairs) is carried out and the gasket frames are installed. Afterwards, the segments are stored in the outdoor storage area in stacks of three segments with intrados up and two wooden bars between the segments. After 28 days, they are transported to the construction site by road. Careful storage and handling of the SFRC segments is important as they are more sensitive than conventional segments.

3.4. Segment erection

It would have been difficult to achieve sufficient safety for the lifting of the segments with a simple lifting pin type erector. The segments are therefore installed with a vacuum pad erector in combination with a 110 mm diameter erector shear pin in a 115 mm deep recess in the centre of the segments. The erector pin takes the shear force of max 89 kN resulting from the segment weight and gasket compression. A larger number of damp stains were detected at the two erector cone recesses in the SFRC segments installed in the 2. Heinenoord tunnel (Kooiman et al., 1999). Erector cone recesses and bolt pockets represent a weakening of the segment cross section and can be a typical location of crack initiation. Furthermore, erector cone recesses are usually aligned with the radial joints of the adjacent rings. This increases the risk of crack initiation in a newly installed segment under the push ram loads in case of misalignment of the two supporting segments of the existing ring. No damp stains have been found at the erector cone recesses in the district heating tunnel. This positive result may be attributed to the fact that the segments are weakened by only one, relatively shallow erector cone recess and that possible local damage during installation has been avoided by the use of a vacuum pad erector.

3.5. Loading by the push rams

The TBM is equipped with 20 push rams equally distributed over the circumference, which transfer their thrust forces on the segments via 45 cm long and 25 cm wide

Please cite this article in press as: Kasper, T. et al., Lining design for the district heating tunnel in Copenhagen, Tunnel. Underg. Space Technol. (2007), doi:10.1016/j.tust.2007.11.001

ram shoes. The maximum ram load per ram shoe has been specified by the manufacturer as 1330 kN. The concentrated loading of the segments causes tensile stresses (bursting stresses) which can lead to cracking as indicated in Fig. 5(left). Considering the section between two symmetry planes as shown in Fig. 5(left), the problem has been investigated by means of a simplified elastic finite element computation as shown in Fig. 5(right). Below the ram shoes the bursting stresses are max 1.6 MPa. At the surface in between the ram shoes they exceed the tensile strength of 4.1 MPa in a zone with a depth of approximately 3 cm. Superficial cracks might occur but have not been observed. It should be noted that the investigated ram load represents a maximum value and the actual average value during construction is approximately 500 kN per ram shoe. If cracks would occur they would be expected to close again when the lining rings are compressed by the grout, earth and groundwater pressure behind the TBM. Steel fibre reinforced concrete is advantageous because steel bar reinforcement is not possible so close to the surface. If uneven support of the newly installed segment by the existing ring leads to large additional bending stresses in the segment, damage is difficult to avoid even with steel bar reinforcement. A crack becomes clearly visible and the segment has to be repaired. This has occurred only a few times.

3.6. Failure of the push rams during installation

It cannot be excluded that the ring installation starts with the first segment at the tunnel crown. If the push rams are by mistake withdrawn from the segment it has to cantilever. This accidental loadcase has been verified by simple hand calculations and testing of the bolt connections. The assumed bearing behaviour is shown in Fig. 6, with Z denoting the tensile force in bolts 2 and 3 and D denoting the compressive force in the concrete contact areas below bolts 1 and 4. The necessary pull-out capacity of the bolts has been determined as 67 kN. The experimentally determined pull-out capacities of min. 130 kN provide a sufficient safety of approximately 2. The shear capacities of the bolts for this situation have also been found to be sufficient with a safety factor of 2.

3.7. Permanent loading without heating of the tunnel

The sectional forces in the tunnel lining for this loadcase have been determined by means of 2D plane-strain drained numerical computations using the finite difference code FLAC (Itasca, 2006). The two models for the deepest and the shallowest section of the tunnel are shown in Figs. 7 and 8, respectively. The displacement boundary conditions consist of horizontal fixities along the vertical model boundaries, vertical fixities along the bottom of the models and rotation fixities of the beam element nodes of the tunnel lining in the vertical symmetry axes. A fine grid is used in the vicinity of the tunnel. The applied material parameters are listed in Table 2. All soil layers have been modelled with the elasto-plastic Mohr–Coulomb model, yet the predicted deformations remain elastic. The grout is considered as an elastic material based on its hardened properties. While the soil layers and the grout are modelled by continuum elements, the tunnel lining is modelled by elastic beam elements with $EI = 85$ MNm^2/m, $EA = 11{,}370$ MN/m considering a Poisson's ratio of 0.17. The tunnel is located completely within the limestone, which is modelled as a homogeneous, isotropic material with equivalent parameters derived from an evaluation and homogenisation of the rock mass properties (Knudsen et al., 1995; Hansen and Foged, 2002; Markussen, 2002; Jackson et al., 2004).

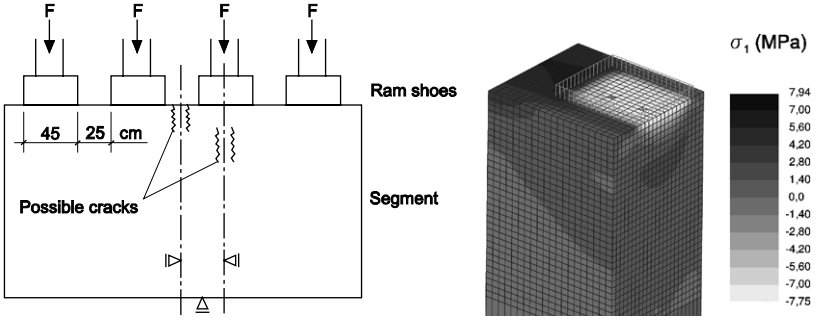

Fig. 5. Loading of the segments by the push rams (left) and computed maximum principal stresses around the ram shoes (right).

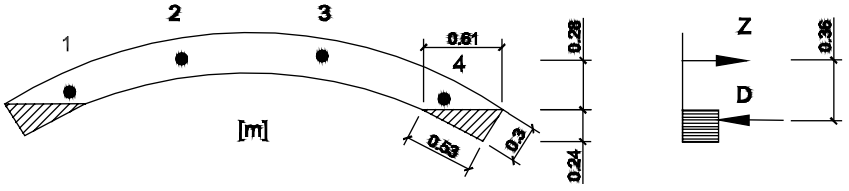

Fig. 6. Assumed bearing behaviour of a segment cantilevering from an existing lining ring.

Please cite this article in press as: Kasper, T. et al., Lining design for the district heating tunnel in Copenhagen, Tunnel. Underg. Space Technol. (2007), doi:10.1016/j.tust.2007.11.001

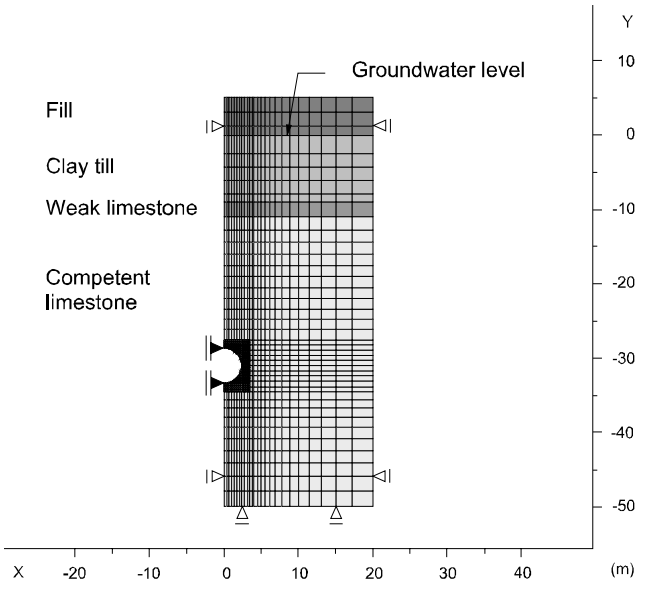

Fig. 7. FLAC numerical model for the deepest section.

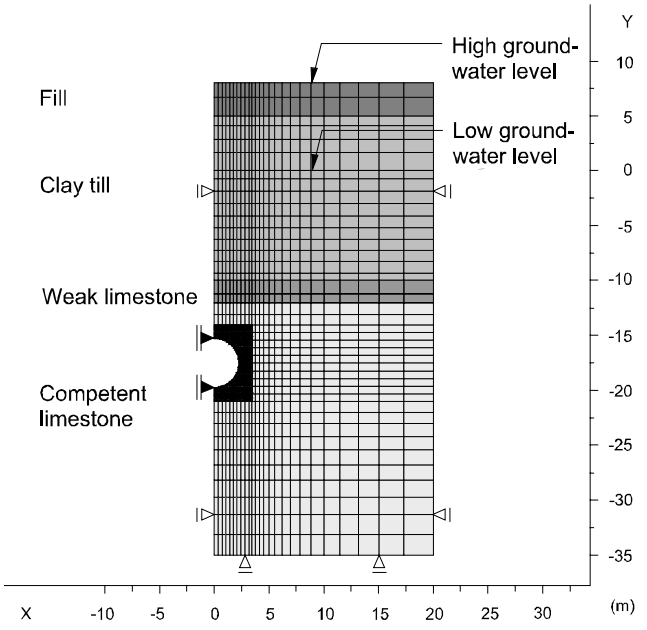

Fig. 8. FLAC numerical model for the shallowest section.

The limestone is actually characterised by a horizontal stratification with layers of different degrees of induration. This results in an anisotropy with a larger stiffness in horizontal direction than in vertical direction. Such an anisotropy in general leads to a larger resistance of the ground to the ovalisation of the tunnel lining and, consequently, leads to smaller bending moments. It has a similar positive effect with regard to the heating of the tunnel. The larger stiffness in horizontal direction leads to a larger horizontal and smaller vertical thermal expansion of the limestone. This results in bending moments in the lining with opposite signs compared to the bending moments due to earth and groundwater pressure. On the whole, the anisotropy of the limestone is not considered unfavourable with regard to the sectional forces in the tunnel lining and is therefore not taken into account in the numerical modelling. As the stiffness of the limestone is one of the key parameters and can have a relatively large variation due to the different degrees of induration, both a lower and upper bound estimate are investigated. The largest loading of the lining occurs at the deepest section of the tunnel with a high groundwater level. On the other hand, the shallow location may be more critical due to the reduced normal forces in the lining ring and possibly higher bending moments. Therefore, both sections have been analysed and the shallow section has been investigated with a high and a low groundwater level.

After having modelled the in-situ stresses and groundwater pressures in a first step, the tunnel construction is simulated in a second step by deactivating the soil elements inside the tunnel, changing the material properties of the limestone elements in the area of the grout from limestone to grout and introducing the beam elements for the lining. This modelling procedure with the tunnel lining 'wished in place' does not consider pre-relaxation of the ground due to tunnel excavation and installation. However, due to the support of the closed tunnel face by the excavated material in the EPB shield machine, due to the long stand-up times of the limestone and high advance rates of the shield machine, and finally due to the fast gelling and hardening of the grout, the pre-relaxation of the ground is deemed small enough to be neglected in the modelling. It should also be noted that an overestimation of the stresses on the lining by the chosen modelling approach gives conservative results. The joints in the lining are not considered, which represents a conservative simplification resulting in an overestimation of the bending moments, whilst the normal forces are not affected by this assumption. Comparative simulations with a circular and a flat, elliptical shape of the tunnel ring are made to consider

Table 2
Material parameters of the different soil layers and the grout

Material	γ (kN/m^3)	E (MPa)	ν (–)	φ' (°)	c' (kPa)	K_0 (–)	k (m/s)
Fill	22	10	0.3	30	0	0.5	
Clay till	23	150	0.3	34	10	0.44	
Limestone crushed zone	22	1000	0.25	45	50	0.29	
Competent limestone	22	1500 (min) 10,000 (max)	0.25	45	100	0.29	1×10^{-6}
Grout	12	1000	0.25				

Please cite this article in press as: Kasper, T. et al., Lining design for the district heating tunnel in Copenhagen, Tunnel. Underg. Space Technol. (2007), doi:10.1016/j.tust.2007.11.001

the specified circle shape tolerance of the lining of $\Delta d = 25$ mm. For the verification of the sectional forces, an additional bending moment of $\Delta M_{\mathrm{Lip}} = 0.015 \cdot \mathrm{N}$ is considered to take into account the specified lipping tolerance of 1.5 cm at the joints. Both ultimate limit state (ULS) and serviceability limit state (SLS) computations are made.

The verification of the bearing capacity of the lining cross section is based on a stress–strain relationship according to the German guideline as shown in Fig. 9. A parabolic-rectangular stress block with the compressive strength f_{cd} is assumed in the compression zone, while a simplified, conservative rectangular stress block with the tensile strength $f_{\mathrm{eq,ctd,II}}$ is assumed in the cracked tension zone (cp. Fig. 4). In tension, tensile strains $\varepsilon_{\mathrm{ct}}^{\mathrm{f}}$ of up to 10‰ are allowed (point A). In compression, compressive strains $\varepsilon_{\mathrm{c}}^{\mathrm{f}}$ of up to $\varepsilon_{\mathrm{c2u}} = -3.5$‰ are allowed (point B). The compressive strength f_{cd} is reached at a compressive strain of $\varepsilon_{\mathrm{c2}} = -2$‰ (point C). A procedure has been implemented into the program MATLAB to determine the M–N failure envelope by means of systematic variations of the strain distributions within the admissible range. Figs. 10 and 11 show the envelopes of the sectional forces and the failure envelopes for the deepest section and for the shallowest section with low groundwater level, respectively. The sectional forces are shown both for the upper and the lower bound estimate of the limestone stiffness. In traditional design models for tunnels (Duddeck and Erdmann, 1982), the dependence of the sectional forces on the stiffness relation between soil and tunnel lining is described

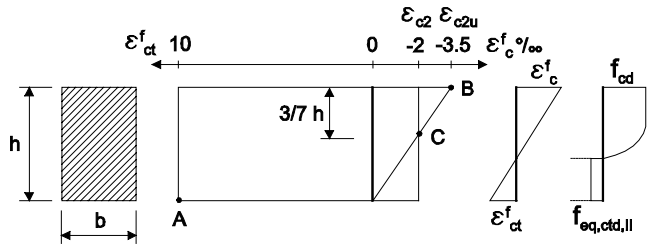

Fig. 9. Rectangular SFRC cross section: definition of admissible strain ranges and assumed, simplified stress–strain relationship for the verification of the bearing capacity.

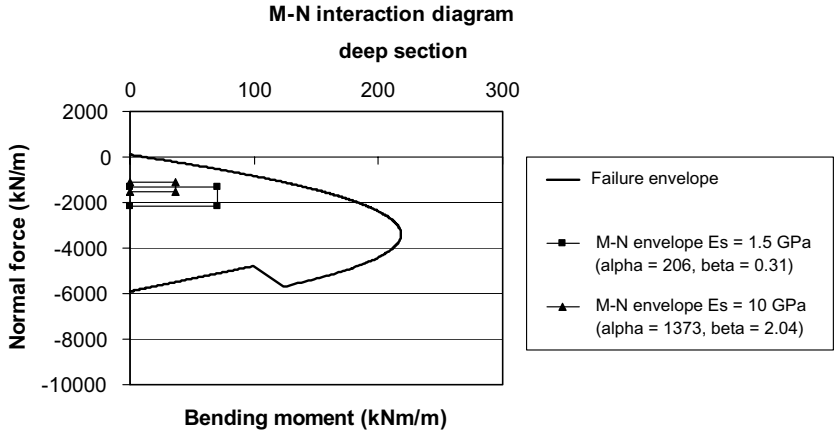

Fig. 10. Failure envelope and envelope of the sectional forces for the deepest tunnel section without heating, for the upper and lower bound estimate of the limestone stiffness E_{s} (stiffness ratios α and β).

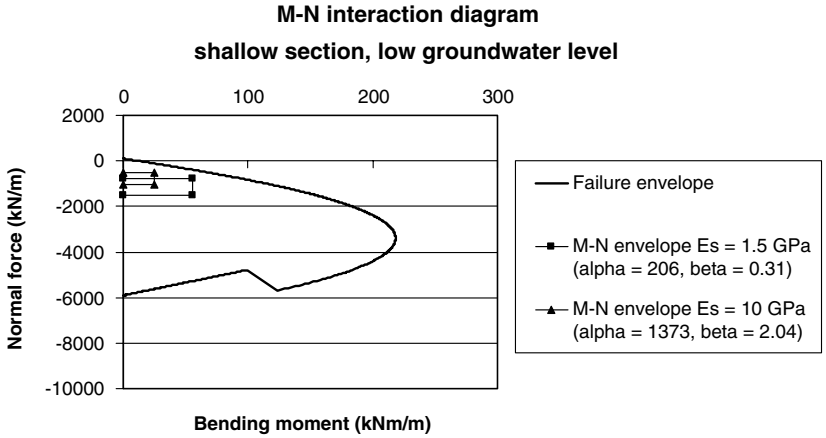

Fig. 11. Failure envelope and envelope of the sectional forces for the shallowest tunnel section with low groundwater level, without heating, for the upper and lower bound estimate of the limestone stiffness E_{s} (stiffness ratios α and β).

Please cite this article in press as: Kasper, T. et al., Lining design for the district heating tunnel in Copenhagen, Tunnel. Underg. Space Technol. (2007), doi:10.1016/j.tust.2007.11.001

by a bending stiffness ratio $\alpha = E_s R^3/EI$ and a compressibility stiffness ratio $\beta = E_s R/EA$. In these formulae, E_s denotes the soil stiffness, R the tunnel radius and EI and EA the section properties of the tunnel lining. In the Figures, the range of the sectional forces is indicated by rectangles, bounded by the lines $\min N$, $\max N$, $\min M = 0$ and $\max M$. The discontinuity in the failure envelope is due to the required higher safety factor of 1.8 for failure of uncracked cross sections compared to 1.25 for failure of cracked cross sections. All sectional forces lie within the failure envelope, i.e. the capacity of the SFRC cross section is sufficient. For the currently considered loadcase of the permanent loading without heating of the tunnel, the shallowest section with low groundwater level is the most critical one (Fig. 11). The SFRC guideline requires a limitation of the crack widths in the ULS to 1/20 of the fibre length = 2.35 mm to ensure sufficient anchorage of the fibres. The cross sections are almost completely in compression and the calculated crack widths are very small. The maximum ULS crack width is obtained for the shallowest section with low groundwater level and is 0.014 mm. The calculated maximum SLS crack width is 0.004 mm.

Similar to the loading of the segments by the push rams (Section 3.5) the concentrated transfer of the forces in the lining ring through the radial joints causes high compressive stresses as well as bursting stresses at the joints. This phenomenon has been investigated experimentally with respect to SFRC segments e.g. by Dupont et al. (2003) and Suter and Bergmeister (2004) and is also addressed e.g. by De Waal (1999) and Woods and Battye (2003). The large ring normal force together with the large bending moment at the deepest section of the district heating tunnel represents the most critical situation. The sectional forces have been transformed into an equivalent triangular contact pressure distribution giving a contact width of 12.8 cm and a peak pressure of 34 MPa in the ULS and 25 MPa in the SLS. The problem has been analysed by a 2D plane-strain FLAC model as shown in Fig. 12. To consider cracking, the concrete is modelled as an elastic–perfectly plastic material with a tension cut-off. The tensile strength (tension cut-off) is taken as $f_{eq,ctd,II} = 0.89$ MPa in the ULS calculation and $f_{ctm} = 4.1$ MPa in the SLS calculation (cp. Fig. 4). The strain level of max 0.5‰ in the cracked areas in the ULS is small, which verifies that $f_{eq,ctd,II}$ can be used. The cracks do not represent a critical failure state and can therefore be accepted. No cracking is predicted in the SLS, as the computed maximum principal tensile stresses of 2.0 MPa remain below the mean tensile strength of the concrete of 4.1 MPa.

3.8. Permanent loading with heating of the tunnel

The pipelines in the tunnel are thermally insulated and the operation of the ventilation system to cool the tunnel has been simulated and optimized with the result of a proposed daily 12 h ventilation during night time (Matlok et al., 2005). The corresponding average heat flux on the inner surface of the tunnel lining is 19.7 W/m^2. The design initial temperatures before heating are 8 °C. The influence of the thermally induced, upward groundwater flow around the tunnel and the general horizontal groundwater flow in the region of the tunnel on the heating induced temperature field has been analysed by poro-hydro-thermal 2D FLAC analyses. All details of these analyses are contained in Kasper (submitted for publication) and are therefore not covered in this paper. It has been found that, for the given low permeability of the limestone and the low horizontal

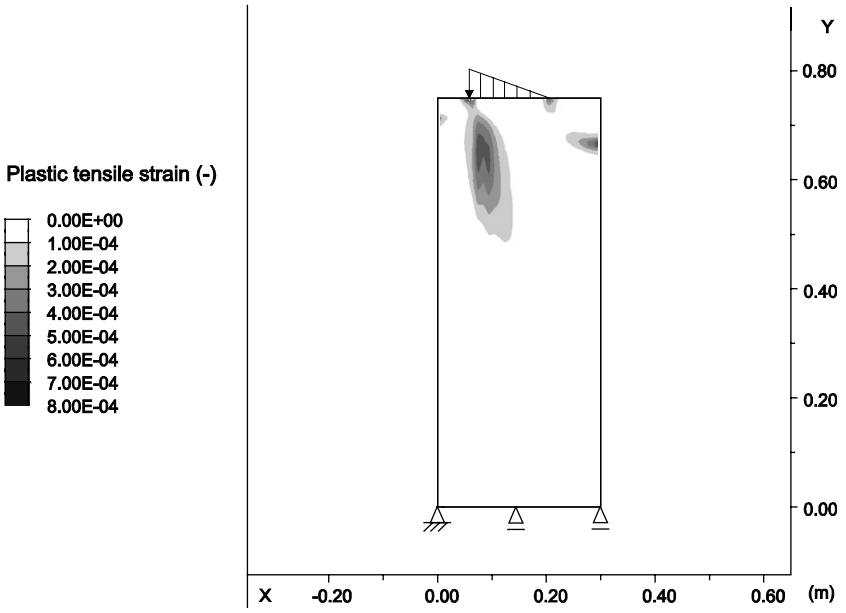

Fig. 12. Computed tensile plastic strains (cracking) at the radial joints for the permanent situation without heating, based on $f_{eq,ctd,I} = 0.89$ MPa (ULS).

Please cite this article in press as: Kasper, T. et al., Lining design for the district heating tunnel in Copenhagen, Tunnel. Underg. Space Technol. (2007), doi:10.1016/j.tust.2007.11.001

groundwater flow velocity perpendicular to the tunnel, the temperature field is simply axisymmetric around the tunnel and corresponds to the pure conduction solution (Figs. 13 and 14). It has further been found that the situation would be different for higher permeabilities of the ground and higher velocities of the horizontal groundwater flow.

Motivated by the results of the studies, the temperature evolution and the corresponding thermally induced deformations and stresses have then been analysed by a simple axisymmetric thermo-mechanical model as shown in Fig. 15. The axis of rotational symmetry is at $x = 0$. The inside of the lining is at $x = 2.1$ m and the outer boundary of the model is chosen at $x = 20$ m. A discretisation with 2×30 elements is used, modelling the tunnel lining by 2×10 elements, the grout by 2×5 elements and the limestone by 2×15 elements. In addition to the mechanical properties (Tables 1 and 2), thermal material parameters are needed for this model and are summarised in Table 3. The parameters of the concrete are common values, while the parameters of the grout and limestone have been estimated from literature, experience and laboratory tests. Starting from an assumed initial, uniform temperature of

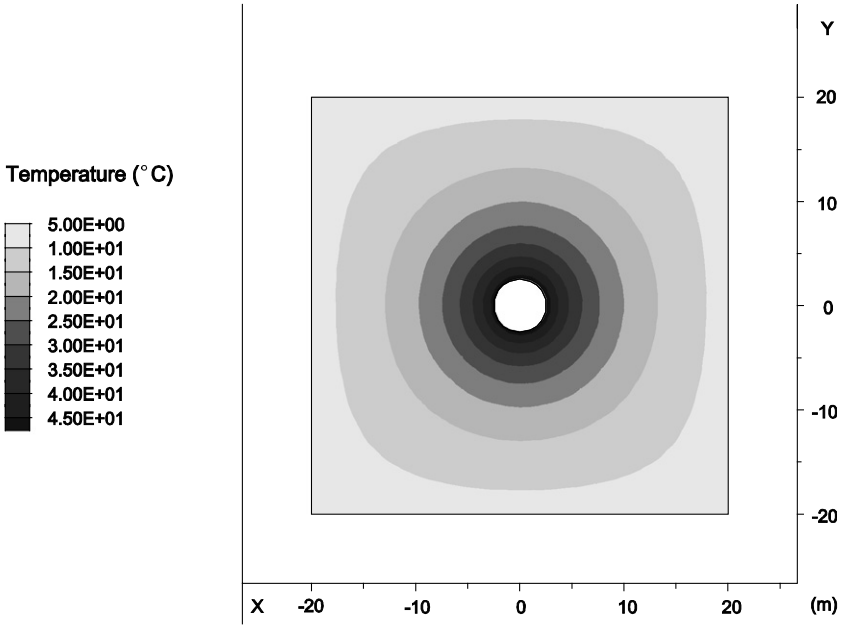

Fig. 13. Computed steady-state temperature field in the limestone (after 5 years).

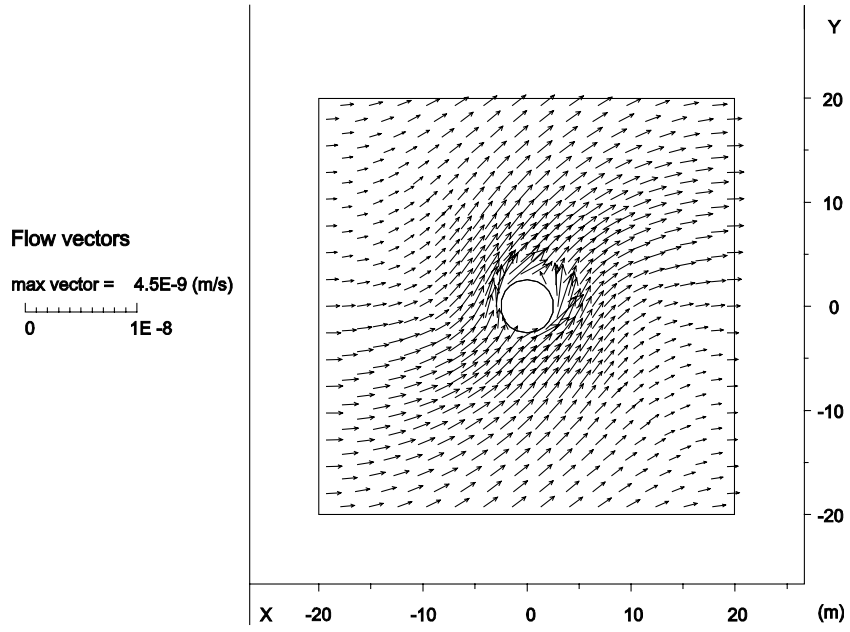

Fig. 14. Computed steady-state groundwater flow in the limestone (after 5 years). The maximum flow velocity is max $q_w = 0.39$ mm/day.

Please cite this article in press as: Kasper, T. et al., Lining design for the district heating tunnel in Copenhagen, Tunnel. Underg. Space Technol. (2007), doi:10.1016/j.tust.2007.11.001

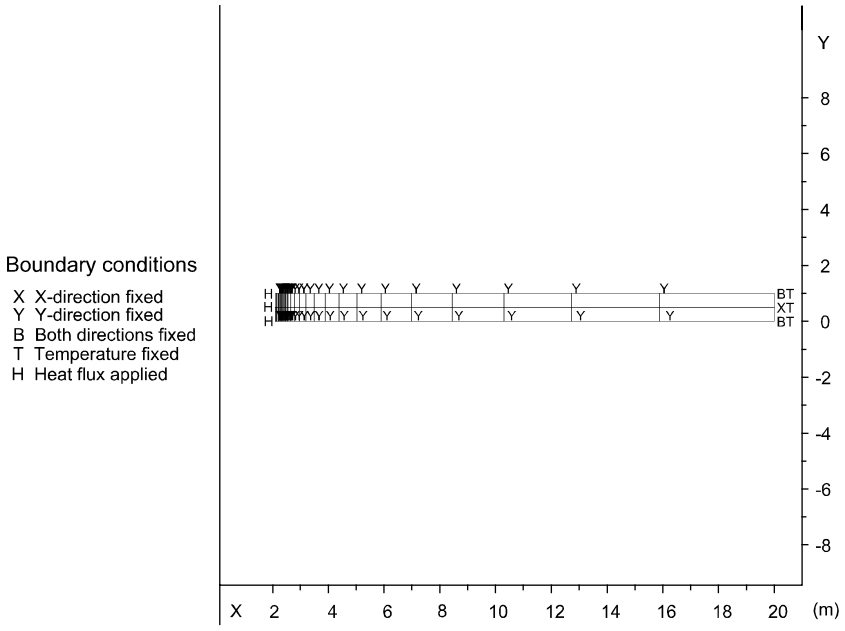

Fig. 15. Axisymmetric thermo-mechanical model for the heating of the tunnel.

8 °C, considering the boundary conditions as shown in Fig. 15 with the heat flux applied on the inside of the lining and performing a thermo-mechanical calculation through time yields the temperature evolution and the corresponding temperature induced deformations and stresses. The computed temperature evolution is shown in Fig. 16. The final steady-state temperature on the inner surface of the lining is 53.3 °C and 49.4 °C on the outside of the lining. Four temperature monitoring sections will be installed in the tunnel to control the predicted temperatures.

The temperature induced tangential stresses in the lining have been integrated to obtain the corresponding sectional forces. Fig. 17 shows the envelope of the sectional forces considering the temperature elevation for the deepest tunnel section. An increase of both the normal force and the bending moment can be observed. The latter is due to the temperature gradient over the thickness of the lining and due to lipping. It can be concluded that the deepest section is the most critical one with regard to the permanent loading situation with heating of the tunnel. All sectional forces lie within the failure envelope, i.e. the capacity of the SFRC cross section is sufficient.

Fig. 18 shows the predicted cracking at the radial joints in the ULS for the permanent situation with heating of the tunnel (cp. Fig. 12 without heating). The situation with heating of the tunnel is clearly worse. However, the strain

Table 3
Thermal parameters of the tunnel lining, grout and limestone

Material	Specific heat (J/(kg K))	Thermal conductivity (W/(m K))	Coefficient of thermal expansion (1/K)
Concrete	900	1.4	10×10^{-6}
Grout	900	1.3	10×10^{-6}
Limestone	1310	1.9	6×10^{-6}

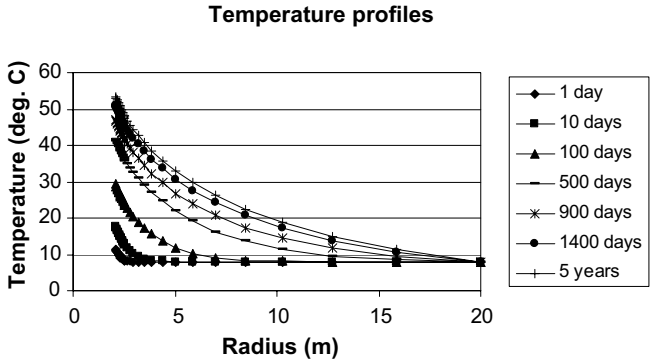

Fig. 16. Computed temperature profiles at different points in time. The steady state is reached after approximately 5 years.

level of max 2.5‰ in the cracked areas is still small. It is concluded that the cracks do not represent a critical failure state and that the integrity of the structure can be maintained by the steel fibres. In an SLS computation, no cracking is predicted as the maximum principal tensile stresses of 3.5 MPa still remain below the mean tensile strength of the concrete of 4.1 MPa.

4. Durability design

The client has required that the heating tunnel shall be designed to satisfy a specific service life of 100 years, where the structure should not require major maintenance and repair. The elevated temperature in combination with the aggressiveness of the environmental exposure requires special attention. The tunnel is located in saline groundwater, mainly close to the harbour with chloride contents of 1–1.5% (close to the seawater the chloride content is about 1.6%). Due to this, the most critical deterioration process

Please cite this article in press as: Kasper, T. et al., Lining design for the district heating tunnel in Copenhagen, Tunnel. Underg. Space Technol. (2007), doi:10.1016/j.tust.2007.11.001

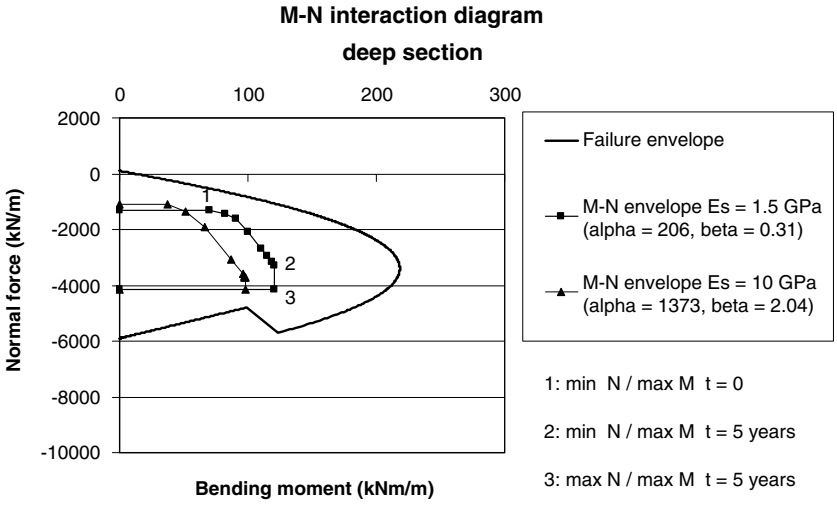

Fig. 17. Failure envelope and envelope of the sectional forces for the deepest tunnel section with heating, for the upper and lower bound estimate of the limestone stiffness E_s (stiffness ratios α and β).

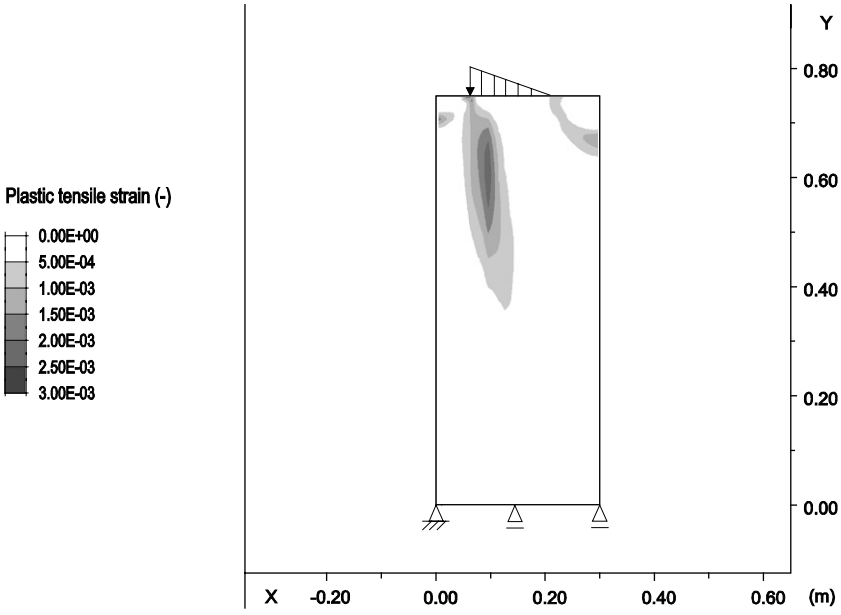

Fig. 18. Computed tensile plastic strains (cracking) at the radial joints for the permanent situation with heating, based on $f_{eq,ctd,I} = 0.89$ MPa (ULS).

in case of traditionally reinforced segments would be chloride induced reinforcement corrosion which, for structures in marine environment, would require special measures to guarantee a service life of 100 years (end of service life is usually defined by the start of reinforcement corrosion). In the present case, the situation is even more serious due to the increased temperature, as the temperature level is decisive for the rate of transporting aggressive substances such as chlorides into and within concrete. All chemical and electro-chemical reactions are accelerated by increase in temperature. According to a simple rule of thumb an increase in temperature by 10 °C causes a doubling of the rate of reaction. In the present case the temperature is approx. 40 °C higher than in usual, bored tunnels with approx. 10 °C, which will lead to a $2^4 = 16$ times faster ingress of chlorides in the heating tunnel compared to the ingress rate in normal, bored tunnels. In addition, the corrosion process may be accelerated due to the risk of accumulation of chlorides at the internal tunnel surfaces due to evaporative effects. These factors would make it very difficult to design the heating tunnel for a 100 years corrosion free service life when trusting alone on the traditional durability measures such as sufficiently large and sufficiently dense concrete layers. In the present case, the traditional design would require covers of approximately 80-100 mm, which is far too high for bored tunnels as they induce a high risk of spalling of the very thick, unreinforced cover during handling and installation of the segments.

Please cite this article in press as: Kasper, T. et al., Lining design for the district heating tunnel in Copenhagen, Tunnel. Underg. Space Technol. (2007), doi:10.1016/j.tust.2007.11.001

Several research investigations (Raupach and Daubenschmidt, 2004; Weydert and Schiessl, 1998) have shown a favourable behaviour of SFRC with respect to durability. This is due to the fact that the critical chloride content of SFRC (so-called threshold value) is much higher than that of normal steel reinforcement, although identical steel compositions are used. Further, the corrosion activity of steel fibre reinforced concrete is very limited and limited to a surface rusting of some protruding single fibres. Although rust spots near the surface may occur, corrosion will not penetrate deeply as a result of the following reasons in case of uncracked concrete:

- Continuous corrosion between individual fibres is not possible because each fibre is individually embedded in and thus protected by the concrete. Therefore, no electrical conduction occurs which would result in a continuous process (no macrocell corrosion possible).
- Surface corrosion near fibres will not cause the concrete to spall. The stresses caused by the expansion of the fibre diameter are negligible and do not lead to more damage.

This means the steel fibre corrosion of uncracked concrete is first of all an aesthetic problem, (however often not relevant for tunnels) and has no influence on the structural behaviour.

The potentials of adopting stainless steel fibre reinforcement will definitely gain more momentum in the future, both on the contractor's side due to the obvious advantages regarding handling and transport, and hopefully also on the designer's side due to the advantage regarding durability.

5. Gasket design

The segments are equipped with EPDM gaskets (Fig. 2). The question was raised if the gaskets remain watertight under 55 °C over 100 years. An accelerated gasket relaxation test with an elevated temperature of 100 °C over 252 days has been made which, according to the Williams–Landau–Ferry (WLF) equation, corresponds to a prediction period of 146 months (12 years) for 55 °C. An extrapolation of the measured data to 100 years gives a residual stress level of about 50%. According to the tightness diagram of the chosen gasket, the tunnel would be watertight even for a relaxation to only 6% residual stress level.

6. Laboratory tests

Mix design, casting technology and quality control are of vital importance for SFRC. The design and segment production required some iterations and optimization and have been accompanied by the following material tests:

- Petrographic analyses on plan-sections of extracted cores to investigate the distribution of the fibres in the hardened concrete. In the beginning, the distribution of the fibres was not always as homogeneous as desirable with some higher amounts of fibres in the lower part of the cores. This concrete test has proven to be very useful and almost indispensable, at least during the pre-testing and starting phase of the production.
- Wash-out tests of fresh concrete to determine the amount of fibres. The intention was to find a simple test method which gives a second control of the actual fibre amount in addition to the automatic weighing determination at the mixing plant.
- 4-Point bending tests to ensure the required strength properties.
- Splitting tests (Brazilian tests) as additional tensile strength tests.
- Unconfined compressive strength tests to ensure the specified C50/60 concrete class.

7. Experiences during segment production and tunnel construction

Mainly at the beginning of the segment production, some small cracks were observed after demoulding at the inner edges of the gasket grooves around the segment corners. It is suspected that this was caused by the interaction of hydration and temperature evolution during curing in the fixed moulds in the production hall within the first 12 h. Cracks smaller than 0.15 mm were repaired by impregnation with low-viscous epoxy resin, which is absorbed into and thus fills the cracks. Segments with cracks larger than 0.15 mm were rejected. SFRC has a higher risk of honeycomb and blow hole formation compared to conventional concrete. Limited defects around the gasket grooves were reworked after demoulding. Segments with defects which could not be repaired (broken edges, larger blow holes and honeycombs) were rejected. After optimization of the production technique and production parameters, the SFRC segments have not shown a larger number or larger size of blow holes and honeycomb defects compared to traditionally reinforced segments. No formation of fibre clusters (balling) has been detected by visual inspection or petrographic analyses.

In the first 2.4 km long section of the tunnel drive, cracks at the corners of key segments have occurred in a larger number of rings. This is most likely caused by thrusting the segment into a too narrow gap between the counter key segments, leading to cracks immediately or later when the ring compression increases just behind the shield tail. This can be avoided more easily in segments with conventional reinforcement by the steel bars in the corner regions. It is interesting to note that the number of these damages has significantly decreased in the second section of the tunnel drive. This is attributed to the typical learning process of the ring installation teams within a project such that finally almost no mistakes occur even with high production rates. A major benefit of using SFRC in the district heating tunnel is the fact that structurally irrelevant minor damages

Please cite this article in press as: Kasper, T. et al., Lining design for the district heating tunnel in Copenhagen, Tunnel. Underg. Space Technol. (2007), doi:10.1016/j.tust.2007.11.001

on the inside of the segments do not have to be repaired. There are no aesthetic concerns, and there is no need to restore a required concrete cover of steel bar reinforcement. Furthermore, a possibly required cathodic protection in case of traditionally reinforced segments with special installations to connect the reinforcement cages of all segments is unnecessary. These facts contribute to the cost-efficiency of the chosen SFRC segment solution.

It can be stated that only a very small number of structural cracks have been detected, which are often observed in other tunnel projects. It is difficult to say if this is due to the use of SFRC (its ductility). However, a favourable ductile behaviour and crack distribution of SFRC has been proven in many tests and reported in the literature. There has been a number of leaking joints and cracks at the corners of key segments, which have been sealed by acrylic-based hydro-structural resin after the tunnel drive. In general, the segments have shown a high quality and have been easy to handle and install in the tunnel, which is deemed to be one of the reasons for high production rates of up to 49.5 m per day.

8. Conclusions

Following a few previous applications in some tunnel projects, the lining for the 3.9 km long district heating tunnel in Copenhagen is made of SFRC segments without conventional steel bar reinforcement. This eliminates the problem of corrosion, ensures the required durability over 100 years under elevated temperatures, enables a cost-efficient segment production and helps to achieve a successful construction with low segment damage rates and repair costs. The client is expected to gain from the use of SFRC by reduced operation and maintenance costs during the life time of the tunnel. The design procedures and tests for the SFRC segments in the district heating tunnel have been described in detail in this paper. Prevailing positive experiences during construction of the tunnel suggest the use of this kind of segments also in future projects.

Fibre reinforced concrete is expected to gain more attention also in view of fire protection. In traditionally reinforced segments without fire protection cladding the temperature increase often requires an increased amount of reinforcement and/or concrete cover (lining thickness). Fire protection cladding on the other hand necessitates a larger opening size, additional maintenance (replacements of the cladding) and makes it difficult to inspect the tunnel lining. The combination of steel fibre and polypropylene fibre reinforcement can provide a fire resistant concrete, which does not require additional measures and saves construction costs.

Steel fibre and polypropylene fibre reinforced concrete segments combined with a two-component grout to avoid the need of shear coupling between the rings is therefore envisioned as an interesting and competitive solution. It represents a simple, cost-efficient, robust and durable system with low maintenance costs.

Acknowledgements

The authors gratefully acknowledge the permission from the client, Copenhagen Energy, to publish this paper.

References

Anonymous, 1995. Steel-fibre-reinforced segments for Heathrow baggage-handling tunnel. Quality Concrete 1 (3), 65–68.

Bezuijen, A., Talmon, A.M., 2003. Grout the foundation of a bored tunnel. In: Proceedings of the International Conference on Foundations ICOF2003, Dundee, UK. Thomas Telford, London.

Davis, H., Woods, E., Shuttleworth, P., 2006. Focusing on fibres: CTRL experience. Tunnels and Tunnelling International 20 (3), 29–32.

Deutscher Beton- und Bautechnik-Verein (DBV), 2001. Guideline Stahlfaserbeton.

De Waal, R.G.A., 1999. Steel fibre reinforced tunnel segments. Ph.D. Thesis, Delft University.

Dobashi, H., Konishi, Y., Nakayama, M., Matsubara, K., Fujii, A., 2006. Development of steel fibre reinforced highly flowable concrete segments and application to construction. Tunnelling and Underground Space Technology 21 (3–4), Special Issue: Safety in Underground Space (CD-ROM Proceedings of the ITA-AITES 2006 World Tunnel Congress, Seoul, Korea).

Duddeck, H., Erdmann, J., 1982. Structural design models for tunnels. In: Jones, M.J. (Ed.), Tunnelling'82. Institution of Mining and Metallurgy, London, pp. 83–92.

Dupont, D., Vandewalle, L., Hemmy, O., Erden, E., Schnütgen, B., 2003. The use of steel fibres as splitting reinforcement in tunnel linings. In: Saveur, J. (Ed.), Reclaiming the Underground Space, vol. 2. Balkema, Lisse, pp. 915–920.

Gettu, R., Barragán, B., García, T., Ramos, G., Fernández, C., Oliver, R., 2004. Steel fiber reinforced concrete for the Barcelona metro line 9 tunnel lining. In: Proceedings of the 6th RILEM Symposium on Fibre-reinforced Concretes (FRC), 20–22 September 2004, Varenna, Italy, RILEM, pp. 141–156.

Hansen, H.K., Foged, N., 2002. Kalkens bjergmekaniske egenskaber. In: Frederiksen, J.K. et al. (Eds.), Ingeniørgeologiske forhold i København. dgf-Bulletin no. 19. Danish Geotechnical Society, pp. 31–34.

Itasca Consulting Group, Inc., 2006. FLAC – Fast Lagrangian Analysis of Continua, version 5.0, User's manuals.

Jackson, P.G., Steenfelt, J.S., Foged, N., Hartlén, J., 2004. Evaluation of bryozoan limestone properties based on in-situ and laboratory element tests. In: Proceedings of the 2nd International Conference on Geotechnical Site Characterization, 19–22 September 2004, vol. 2, Porto, Portugal, pp. 1813–1820.

Kasper, T., Meschke, G., 2006a. On the influence of face pressure, grouting pressure and TBM design in soft ground tunnelling. Tunnelling and Underground Space Technology 21 (2), 160–171.

Kasper, T., Meschke, G., 2006b. A numerical study of the effect of soil and grout material properties in shield tunnelling. Computers and Geotechnics 33, 234–247.

Kasper, T., submitted for publication. Poro-hydro-thermal analyses of heat transport in the limestone around the district heating tunnel in Copenhagen. In: 12th International Conference of IACMAG, Goa, India.

King, M.R., 2005. The design of steel fibre reinforced concrete segments. In: Hutton, J.D., Rogstad, W.D. (Eds.), RETC Proceedings 2005. Society for Mining, Metallurgy and Exploration, pp. 936–946.

Knudsen, C., Andersen, C., Foged, N., Jakobsen, P.R., Larsen, B., 1995. Stratigraphy and engineering geology of København Limestone. In: Proceedings of XI ECSMFE, Copenhagen, Denmark. dgf-Bulletin no. 11, Vol. 5. Danish Geotechnical Society, pp. 117–126.

Kooiman, A.G., 2000. Modelling steel fibre reinforced concrete for structural design. Ph.D. thesis, Delft University.

Please cite this article in press as: Kasper, T. et al., Lining design for the district heating tunnel in Copenhagen, Tunnel. Underg. Space Technol. (2007), doi:10.1016/j.tust.2007.11.001

Kooiman, A.G., van der Veen, C., Djorai, M.H., 1999. Steel fibre reinforced concrete segments in the second Heinenoord tunnel. In: fib Symposium Prague, Czech Republic, 13–15 October 1999.

Maidl, B., 1995. Steel Fibre Reinforced Concrete. Ernst & Sohn, Berlin.

Markussen, L.M., 2002. Grundvandsforhold i København. In: Frederiksen, J.K. et al. (Eds.), Ingeniørgeologiske forhold i København. dgf-Bulletin no. 19. Danish Geotechnical Society, pp. 165–182.

Matlok, S., Hansen, B., Frederiksen, M., 2005. Cooling of concrete lining in a district heating tunnel. Proceedings of the International Conference on Tunnel Design and Systems Engineering, 12–13 September 2005, Basel, Switzerland. Independent Technical Conferences Ltd., Kempston, pp. 155–164.

Molins, C., Aguado, A., Marí, A.R., 2006. Quality control test for SFRC to be used in precast segments. Tunnelling and Underground Space Technology 21 (3–4), Special Issue: Safety in Underground Space (CD-ROM Proceedings of the ITA-AITES 2006 World Tunnel Congress, Seoul, Korea).

Moyson, D., 1995. The construction of a steel fibre reinforced concrete segmental lining in London. In: Weltneuheiten im Tunnelbau. Proceedings of the World Tunnel Congress/STUVA-Tagung'95 Stuttgart, Germany. Alba, Düsseldorf, pp. 274–278.

Nymann, J., Taylor, S.D., 2003. Construction of the Copenhagen metro. In: Saveur, J. (Ed.), (Re)claiming the Underground Space, vol. 2. Balkema, Lisse, pp. 607–612.

Plizzari, G.A., Tiberti, G., 2006. Steel fibres as reinforcement for precast tunnel segments. Tunnelling and Underground Space Technology 21 (3–4), Special Issue: Safety in Underground Space (CD-ROM Proceedings of the ITA-AITES 2006 World Tunnel Congress, Seoul, Korea).

Raupach, M., Dauberschmidt, C., 2004. Corrosion behaviour of steel fibres in concrete containing chlorides. In: Long Term Prediction and Modelling of Corrosion. Proceedings of the EUROCORR 2004, European Corrosion Conference, 12–16 September 2004, Nice, France.

Suter, R., Bergmeister, K., 2004. Tübbinge aus Stahlfaserbeton. Beton- und Stahlbetonbau 99, 858–864.

Talmon, A.M., Bezuijen, A., 2006. Grouting the tail void of bored tunnels: the role of hardening and consolidation of grouts. In: Bakker, K.J., Bezuijen, A., Broere, W., Kwast, E.A. (Eds.), Geotechnical Aspects of Underground Construction in Soft Ground. Taylor & Francis, Leiden, pp. 319–325.

Viljoen, B.C., Neumann, M.J.E., Kubisch, F., 1995. Steel fibre reinforced concrete for precast tunnel segments – mix design and full scale testing. In: Weltneuheiten im Tunnelbau. Proceedings of the World Tunnel Congress/STUVA-Tagung'95 Stuttgart, Germany. Alba, Düsseldorf, pp. 279–290.

Wallis, S., 1995. Steel fibre developments in South Africa. Tunnels and Tunnelling International 27 (3), 22–24.

Warren, C., Wittneben, G., Gallagher, M., 2003. C320 – tunnelling under the Thames. Tunnels and Tunnelling International 35 (9), 34–37, Supplement CTRL Section 2 Tunnelling.

Weydert, R., Schiessl, P., 1998. Corrosion of steel fibres in cracked and uncracked steel fibre reinforced concrete. In: Research report no. 516, University of Aachen (ibac), Germany.

Woods, E., Battye, G., 2003. Design decisions for CTRL 2's bored tunnels. Tunnels and Tunnelling International 35 (9), 8–10, Supplement CTRL Section 2 Tunnelling.

Woods, E., Shuttleworth, P., Fesq, C., 2005. Steel fibre reinforced tunnel linings. In: Hutton, J.D., Rogstad, W.D. (Eds.), RETC Proceedings 2005. Society for Mining, Metallurgy and Exploration, pp. 947–956.

Please cite this article in press as: Kasper, T. et al., Lining design for the district heating tunnel in Copenhagen, Tunnel. Underg. Space Technol. (2007), doi:10.1016/j.tust.2007.11.001